Available online at www.sciencedirect.com
ScienceDirect
Surface Science 600 (2006) 3762–3765
SURFACE SCIENCE
www.elsevier.com/locate/susc

Structural and surface analysis of thin-film ZnTe formed with pulsed-laser deposition

Artur Erlacher [a,b,*], Alejandra R. Lukaszew [c], Herbert Jaeger [d], Bruno Ullrich [a]

[a] *Centers for Materials and Photochemical Sciences, Department of Physics and Astronomy, Bowling Green State University, Bowling Green, OH 43403-0224, USA*
[b] *Institut für Experimentalphysik, Karl-Franzens Universität Graz, A-8010 Graz, Austria*
[c] *Department of Physics and Astronomy, University of Toledo, Toledo, OH 43606, USA*
[d] *Department of Physics, Miami University, Oxford, OH 45056, USA*

Available online 21 April 2006

Abstract

Nanosecond pulses of a Nd:YAG laser have been employed to deposit thin-film zinc telluride (ZnTe) on silicon (Si) and glass without heating these substrates. We present and discuss the structural and surface properties of films deposited at 1064 nm and 532 nm. X-ray diffraction and analysis of the surface roughness with atomic force microscopy reveal that the material texture and surface morphology depend on the ablation laser line used rather than on the substrate. The observations contribute to improved understanding of pulsed-laser deposition and provide tools to optimize the optoelectronic and photonic properties of ZnTe thin-films as well as their incorporation into Si-based technologies in order to fabricate cost-effective and functional optoelectronic devices and all-optical laser digitizer.

Keywords: Zinc telluride; Pulsed-laser deposition; X-ray diffraction; Atomic force microscopy

1. Introduction

The II–VI semiconductor ZnTe is a very attractive host for optoelectronic device realizations because of its direct bandgap in the green spectral range (2.26 eV). Specifically, for bright light emitting diodes (LEDs), ZnTe is an interesting candidate since the emission wavelength corresponds to the maximum sensitivity of the human eye. Employments of ZnTe were reported by the realization of LED prototypes [1,2], high-efficiency multi-junction solar cells [3], and terahertz (THz) devices [4,5]. The exploration of novel solutions for future light-based communication systems, such as all-optical switches and hybrid device structures [6], have been the driving motivation for the current work. In our former studies we introduced the concept of laser crossing and all-optical laser transmission digitizing with GaAs [7,8], CdS [9] and InP has been demonstrated [10]. In Fig. 1, photonic digitizing with thin-film ZnTe on glass is shown. The experiment was performed in a similar way as with GaAs (Refs. [7,8]) by switching red (633 nm) laser emission with a green (530 nm) laser. The achieved switch amplitude was 11%.

The hetero-pairing of ZnTe and Si is quite a challenge due to the considerable lattice mismatch of 12% and different bonding natures (ionic vs. covalent) of the materials. Known methods to form ZnTe thin films are molecular beam epitaxy (MBE) [11]. metal-organic vapor phase epitaxy (MOVPE) [12], metal-organic chemical vapor deposition (MOCVD) [6], and electrochemical deposition [13]. The formation of ZnTe thin-films with pulsed-laser deposition (PLD) was studied during the last decade using glass, GaAs or Si wafers as substrate materials [14–16]. These studies primarily focus on the crystalline phase and doping properties of PLD ZnTe films using pulsed lasers at 248 nm [14], 694 nm [15], and 532 nm [16]. When we started ZnTe PLD in 2004, we did not find reports on infrared (IR) ZnTe

* Corresponding author.
E-mail address: erlacher@kotta-labs.bgsu.edu (A. Erlacher).

0039-6028/$ - see front matter © 2006 Published by Elsevier B.V.
doi:10.1016/j.susc.2006.02.061

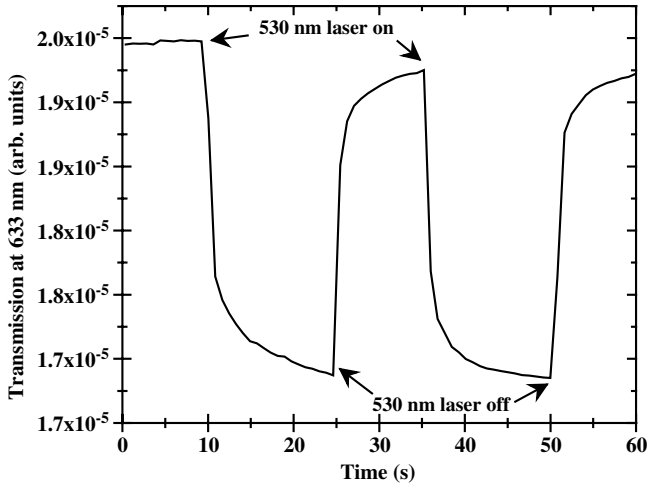

Fig. 1. All-optical switch using ZnTe/glass sample as switching element. A 530 nm laser beam switches a 633 nm laser beam.

PLD. Recently, we presented the optical and optoelectronic differences of ZnTe PLD on glass at 532 nm and 1064 nm [17]. In the current paper, we systematically investigated the crystal and surface features of PLD ZnTe on Si and glass employing ablation wavelengths in the visible and near infrared spectral range.

2. Experimental

ZnTe/glass and ZnTe/Si samples have been formed with PLD using either the fundamental (1064 nm) or second harmonic (532 nm) emission of a Q-switched Nd:YAG laser (6 ns, 10 Hz). The optical penetration depth ($L_0 =$ 1/absorption coefficient) for 1064 nm and for 532 nm is 2 mm and 300 nm, respectively. Since L_0 differs significantly for each wavelength, the energy transfer into the target varies and, as a consequence, different ablation mechanisms are expected. In spite of the laser wavelength variations, all four films were formed in the same way. The four 9's target pellet was formed from hot pressed ZnTe powder and provided by Target Materials Inc, Ohio. The laser spot was adjusted in such a way that the ZnTe target was exposed to a fluence of 0.72 ± 0.04 J cm^{-2}. The target rotated with six revolutions per minute to maintain uniform ablation and to avoid holes. The substrates were either prime grade Si wafers (50.8 mm diameter, (100) orientation) or glass slides (12.7 mm × 12.7 mm × 0.74 mm, industrial grade fused silica). These two substrate materials were chosen to investigate the film growth on either crystalline or amorphous texture. During the deposition the substrate was mounted 60 mm from the target.

All-optical laser digitizer relies on the electronic material alteration in the spot of laser crossing [7,8]. Films deposited on cold substrates increases the ease of optically induced electronic state alterations owing to the expected low order texture. Hence, we deposited the films without the use of a substrate heater. However, increase of the substrate surface temperature is caused by condensation of the impinging particles and blackbody radiation from the PLD plasma. Since nitrogen is known to cause p-type doping of ZnTe [14] we avoided the exposure of the growing film to oxygen–nitrogen complexes by forming the films in a vacuum below 10^{-6} Torr. The deposition of the films took place for 60 min resulting in a thickness of approximately 2 μm according to the deposition rates. The thickness was also verified using the spacing of the transmission interference fringes [18] of the ZnTe/glass samples in the near IR spectrum.

3. Results and discussion

Fig. 2 shows the PLD rates vs. fluence for the employed laser lines. The deposition rates were measured with a quartz crystal thickness monitor and revealed that after overcoming the desorption threshold of 0.1–0.2 J cm^{-2}, the deposition rates linearly increase with the fluence. The deposition rate for 532 nm reaches its maximum at about 1.0 J cm^{-2}. At a fluence above 1.0 J cm^{-2}, the deposition rate decreases because the impact of the incoming laser pulse is reduced by Bremsstrahlung [19] absorption and, in addition, reflection and scattering on particles in the plume (especially such as clusters) lower the effective laser power reaching the target [20]. At 1064 nm, the overall deposition rate is lower and the deposition maximum is notably shifted to 1.5 J cm^{-2}. The shift of the deposition characteristics towards higher fluencies takes place because IR emission is absorbed significantly less by the target and a higher fluence is necessary to reach the required energy density for ablation. With respect to the visible laser line, at 1064 nm, the contribution of thermal desorption to the material ablation is increased and shielding of the target does not occur due to Bremsstrahlung but mainly due to scattering processes in the plume shifting the deposition maximum to higher fluencies and lower the deposition rate below that of the 532 nm line at fluencies beyond 2.5 J cm^{-2}.

The crystallographic properties of the samples and the target were investigated with a Rigaku X-ray diffracto-

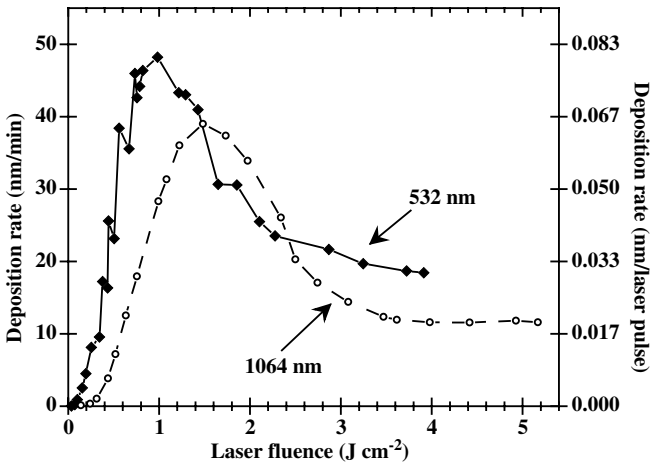

Fig. 2. Deposition rates vs. laser fluence of ZnTe PLD at 1064 nm and 532 nm. The lines are guides for the eyes.

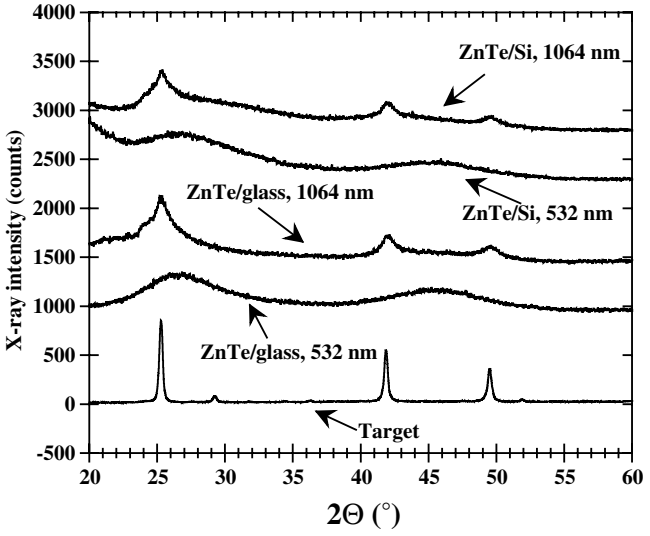

Fig. 3. X-ray diffraction patterns of ZnTe/Si, ZnTe/glass, and ZnTe target. For clarity, the spectra are shifted and the intensity of the target is scaled down.

meter (θ–2θ geometry) using the CuKα line at 0.154054 nm. The X-ray patterns of the samples and the target are shown in Fig. 3. The full widths at half maximum (FWHM) of the observed features are several degrees pointing to a predominantly amorphous film texture. It is known that the growth of ZnTe at room temperature or lower temperatures (100 K) [21] results in amorphous films. The X-ray peak assignments, which have been found in the American Society for Testing and Materials (ASTM) reference, of the samples and the polycrystalline target are summarized in Table 1. The samples formed at 1064 nm show similarity to the target patterns with fairly narrow FWHMs indicating a longer range lattice order than the films ablated at 532 nm. The peak positions at 25.3°, 41.6°, and 49.6° are assigned to the (111), (220), and (311) orientations of the zincblende structure. At a first glance, it seems possible that the peaks at around 45° of the samples formed at 532 nm are the superposition of the peaks at 41.6° and 49.6° of the 1064 nm sample. However, it is more likely that the feature represent a broad (103) peak of the wurtzite structure because peak superposition in amorphous tex-

Table 1
Assignments of the X-ray peaks of the ZnTe/Si samples with the ZnTe literature data

Sample 1064 nm	Sample 532 nm	ZnTe target	Zincblende phase [23]
25.3°	26.6°	25.28°	25.26° (111)
		29.26°	29.25° (200)
41.6°		41.86°	41.80° (220)
	45.3°		45.38° (103) Wurtzite [24]
49.6°		49.50°	49.50° (311)
		51.84°	51.85° (222)
		60.64°	60.63° (400)
		66.76°	66.745° (331)
		76.38°	76.399° (422)

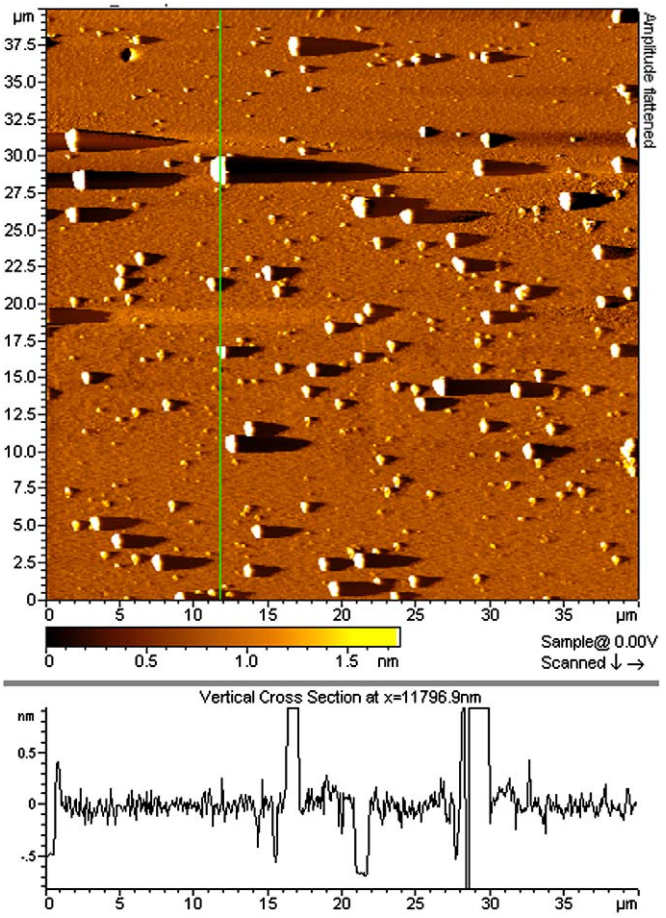

Fig. 4. Surface image and profile of the ZnTe/Si sample formed at 532 nm.

tures is very unlikely since the considerable decrease in the X-ray intensity would prevent noticeable links between X-ray features. It is worthwhile to stress at this point that the X-ray features of the films formed at 532 nm and at 1064 nm in Fig. 3 are identical with those achieved with ZnTe on glass. Thus, the texture of the films does not depend on the provided surface morphology. The same phenomenon has been observed with GaAs PLD on Si and on glass [22].

Atomic force microscopy (AFM) surface images of ZnTe/Si formed at 532 nm and 1064 nm are depicted in Figs. 4 and 5. Similar results have been achieved using glass substrates [17]. The surface of the films formed at 532 nm is covered with clusters, while the underlying texture is very smooth. On the other hand, the film deposited at 1064 nm presents an overall more rough appearance due to a higher density of smaller clusters. We think that the merger of clusters causes the rough underlying structure. Therefore, since clusters improve the local order of the film, the sample formed at 1064 nm possesses improved crystallographic features. Most likely, the increased penetration depth into the target at 1064 nm (in comparison to the highly absorbed 532 nm) causes enhanced cluster ablation, resulting in the film texture shown in Fig. 5. A further possible scenario,

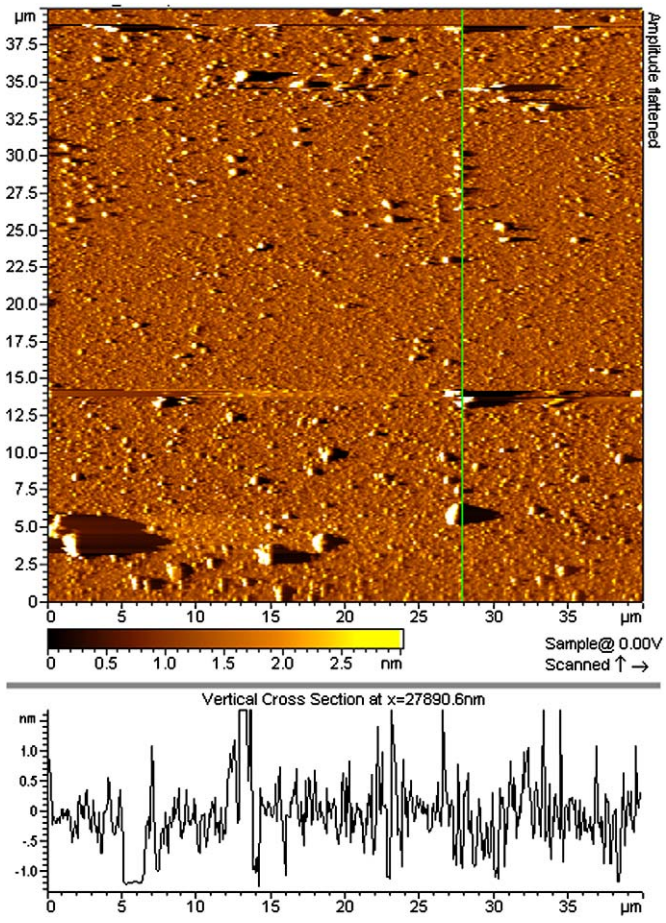

Fig. 5. Surface image and profile of the ZnTe/Si sample formed at 1064 nm.

which might cause a different agglomeration of the material, is the variation of the substrate surface temperature for the two laser emissions used.

4. Summary

Summarizing, we formed thin-film ZnTe on Si and glass with low-temperature nanosecond PLD at 532 nm and 1064 nm. The films produced with the visible irradiation showed an amorphous texture with a smooth surface. At 1064 nm, rougher film surfaces but clearly improved crystal orders were achieved. The results point to intrinsic surface smoothing mechanism of highly absorbed laser ablation lines owning most likely to plume annealing. Furthermore, the results stress the capability of IR PLD to form polycrystalline ZnTe materials without substrate heating and post-annealing. The successful demonstration of straightforward PLD of ZnTe is of importance for industrial thin-film applications. Based on the presented results, it is significant to focus future activities on IR PLD with various target-to-substrate distances and laser fluencies in order to figure out the optimized low-temperature PLD parameters for the formation of the ZnTe/Si hetero-pairing.

Acknowledgements

Acknowledgement is made to the National Science Foundation (#HER-0227899, Northwest Ohio Partnership on Alternative Energy), to the donors of American Chemical Society Petroleum Research Fund for partial support of this research, to the Ohio Board of Regents (OBOR Technology Innovation Enhancement Grants, PI Ullrich), and the McMaster Endowment. We are very thankful to Jonathan Skuza for his assistance during the AFM experiments.

References

[1] K. Yoshino, A. Memon, M. Yoneta, K. Ohmori, H. Saito, M. Ohishi, Phys. Status Solidi (B) 229 (2002) 977.
[2] K. Sato, M. Hanafusa, A. Noda, A. Arakawa, M. Uchida, T. Asahi, O. Oda, J. Cryst. Growth 214/215 (2000) 1080.
[3] D. Rioux, D.W. Niles, H. Hochst, J. Appl. Phys. 73 (12) (1993) 8381.
[4] C. Winnewisser, P. Uhd Jepsen, M. Schall, V. Schyja, J. Helm, Appl. Phys. Lett. 70 (1997) 3069.
[5] K. Liu, H. Kang, T. Kim, X.-C. Zhang, Appl. Phys. Lett. 81 (2002) 4115.
[6] C.X. Shan, X.W. Fan, J.Y. Zhang, et al., J. Vac. Sci. Technol. A—Vac. Surf. Films 20 (6) (2002) 1886.
[7] A. Erlacher, B. Ullrich, Semicond. Sci. Technol. 19 (3) (2004) L9.
[8] B. Ullrich, A. Erlacher, E.O. Danilov, Semicond. Sci. Technol. 19 (12) (2004) L111.
[9] A. Erlacher, H. Miller, B. Ullrich, J. Appl. Phys. 95 (5) (2004) 2927.
[10] A. Erlacher, B. Ullrich, R.J. Konopinski, H.J. Haugan, Proc. SPIE 5723 (2005) 179.
[11] J.H. Chang, T. Takai, B.H. Koo, J.S. Song, T. Handa, T. Yao, Appl. Phys. Lett. 79 (2001) 785.
[12] T. Tanaka, K. Hayashida, S. Wang, Q. Guo, M. Nishio, H. Ogawa, J. Cryst. Growth 248 (2003) 43.
[13] T. Ishizaki, T. Ohtomo, A. Fuwa, J. Phys. D 37 (2004) 255.
[14] C.M. Rouleau, D.H. Lowdnes, Appl. Surf. Sci. 127–129 (1998) 418.
[15] S. Bhunia, D.N. Bose, Solid State Phenom. 55 (1997) 43.
[16] Y. Rajakarunanake, Y. Luo, A. Aydinli, N. Lavalle, A. Compaan, Mater. Res. Soc. Symb. Proc. 268 (1992) 229.
[17] A. Erlacher, M. Ambrico, G. Perna, L. Schiavulli, T. Ligonzo, H. Jaeger, B. Ullrich, Appl. Surf. Sci. 258 (2005) 402.
[18] H. Kuzmany, Solid-State Spectroscopy: an Introduction, Springer, Berlin, New York, 1998, p. 79.
[19] J.C. Miller, R.F. Haglund, Laser Ablation and Desorption, Academic Press, San Diego, 1998, p. 187.
[20] O. Auciello, J. Dordrecht, Multicomponent and multilayered thin-films for advanced microtechnologies: techniques, fundamentals, and devices, Kluwer Academic, Boston, 1993, p. 181.
[21] C.J.L. Moore, D.E. Brodie, Can. J. Phys. 60 (1982) 340.
[22] A. Erlacher, M. Ambrico, G. Perna, L. Schiavulli, T. Ligonzo, H. Jaeger, B. Ullrich, Proc. SPIE 5850 (2004) 1.
[23] ASTM X-ray powder data 15-746.
[24] ASTM X-ray powder data 19-1482.